Chapter 4

Design of 3-D MEMS-Mender Antenna for System in Package Application

An electrically 3D MEMS-Meander Monopole Antenna is presented in this chapter. The design is based on meandered line principle with three-dimensional structure to achieve a reduced size compared to many small printed antennas. This 3D MEMS antenna was demonstrated using MEMS fabrication technique for via holes drilling on glass wafer. However, it can also be fabricated on a silicon substrate and be integrated with the CMOS process. The novel design features the operating frequencies at 2.45GHz with bandwidth 190MHz for 802.11b application.

4-1. Introduction

In recent years, small antenna has become a popular subject in antenna research. Some wireless applications have to be compact enough for convenient carrying and the only way to achieve this demand is to downsize the circuits. It is inevitable to reduce the size of the antenna whose size is much larger than any other parts. To meet these requirements, various kinds of structures and fabrication technologies are investigated and developed, such as meandered antenna [1] for broadband application, fractal antenna [2] and the shorting-posts [3] for miniaturization of the dimensions; or the MEMS technologies [4] for monolithic integration. However, the antennas

mentioned above are not easy to select the position of the slots, and the longitudinal size is still large.

The idea of integration antennas into system in package in currently receiving much attention to further reduce the size and lower manufacturing costs. The through wafer interconnection technology has raised more and more attentions on microelectromechanical systems (MEMS) packaging, radio frequency (RF) circuits, print circuit boards (PCBs) and integrated circuits (ICs) applications [5]~[9]. The major advantages of the through-wafer interconnections are: (1) providing a short interconnection path and hence result in the ground inductance reduction, less signal delay, less noise and less power consumption, (2) increasing the density of the circuits, (3) offering a direct path to the ground and hence increasing the flexibility and density of the chip packaging.

The study of the formation of the through-wafer interconnections has been completed by some researchers [10]~[12]. The through-hole drilling now is gradually becoming a mature technology and can be accomplished by anisotropic wet etching, deep reactive ion etching (DRIE), excimer laser drilling and so on. Anisotropic wet etching is the easiest way for the formation of the through-hole, DRIE has the advantage of high compatibility with standard IC process, and excimer laser drilling can be used in wide range various substrates.

The filling of the through-holes can be realized by polysilicon chemical vapor deposition (CVD) systems [10] or copper electroplating technique [11]~[12]. CVD systems and copper electroplating technique have been widely used in standard IC process with the ability of conformal coating and hence suitable for via filling. One can accomplish the formation of through-wafer interconnections by different combination of drilling and filling technologies.

In this chapter, an idea of applying the micro-electro-mechanical system (MEMS) technologies to fabricate a compact, high performance, and low cost 3D monopole antenna was proposed and studied. The coplanar waveguide (CPW)-fed configuration was used owning to its simple structure, wide bandwidth, and ability of multi-band operation. In order to reduce the size, the meandered monopole antenna was fabricated on both sides of a Pyrex 7740 glass wafer, and the metal lines were connected through via holes, as shown in Fig. 4-1. The A_rF excimer laser micromachining technique for via holes formation was used in this study. Entire antenna was constructed with electroplated thick copper to lower its total resistance, and hence enhanced its performance.

4-2. Design and Fabrication

4-2.1 Antenna Design

Monopole antenna has been widely used in mobile communication systems because of its simple structure and omni-directional radiation pattern. Besides, the meandered pattern layout has often been adapted to enlarge the current path and control the distribution of the electromagnetic (EM) field of the antenna hence the required size of the antenna for a fixed operating frequency can be reduced. Furthermore, due to the fact that current distribution of the antenna affects its radiation pattern, the geometric shape and dimension can be tuned and calculated by means of the simulation tools to get better radiation performance. The coplanar waveguide (CPW)-fed configuration was used for its simple structure, wide bandwidth, and ability of multi-band operation.

The schematic diagram and topology of the proposed 3D meander antenna were shown in Fig. 4-1 [13]. It was fabricated in the form of a microstrip monopole folded on the upper and bottom surfaces of the microwave substrate. The main configuration consists of a feed point and an antenna embodiment. The radiated coils of the antenna are connected to each other in series form by using via holes. Due to its 3D structure, the field analysis of the 3D monopole antenna was very complicate and difficult. Hence, the design analysis and simulation is performed using IE 3D and HFSS by FEM (Finite Element Method).

The proposed antenna was constructed by 15 μm-thick, 1 mm-width cooper lines which folded on both the top and bottom surfaces of the glass substrate, which has the dielectric constant, ε_r = 4.6, and thickness, H = 0.5mm. When H is very small, the electric length will be neutralized. The effect of the height is stronger than parameter S. The geometric length of the antenna, L, is 21 mm, D = 3.85 mm is the width of the antenna, W = 1.5 mm is the spacing between two stripe lines, and S = 1.92 mm for achieving specified total radiating length. The simulation of the 3D monopole antenna was shown in Fig. 4-2 and this proposed antenna was designed for the operation frequency 2.45 GHz. The radiation current distribution is along the longitudinal direction and hence excites the normal mode. Note that the resonant length or the total length of the antenna is larger than one-quarter wavelength of the operating frequency. This is because that the electromagnetic coupling effect between two meandered sections reduces the effective length of the resonant path [14]. The radiation patterns on X-Y, X-Z and Y-Z planes of the proposed antenna are also been simulated. From the simulated results, we can predict that the 3D monopole antenna has the omni-directional radiation pattern which is similar to a monopole antenna with z-axial orientation.

Based on the simulation results, we found that: (1) As the total length increased, the resonant frequency of the antenna dropped. (2) For fixed total length of the antenna, larger value of D will cause the decrease of the resonant frequency and bandwidth of the antenna. This might be due to the larger electromagnetic coupling effect as the value of D increased. (3) For fixed total length of the antenna, the line width of the antenna had slight effect on resonant frequency. It might be due to the impedance mismatch as the line width of the antenna changed.

4-2.2 Antenna fabrication

The details of the fabrication processes of the proposed antenna are shown in Fig. 4-3. The anodically bondable glass wafers, such as Prylex glass, have been chosen to serve as the substrates in our study since they can combine with the silicon technology by means of wafer bonding technology. Besides, compared with silicon substrate, due to the higher resistivity of the glass wafer, the leakage currents at high frequency will be lower hence better performed antenna can be achieved. The A_rF excimer laser which is now commercial available was used for via holes drilling. After via holes drilling, the glass wafer was bonded with a photoresist (PR) layer (AZ 9260, 5 μm) to a temporal substrate which can be reused. The bonded glass wafer was baked on the hot plate at 90 ℃ for 5 minutes. Note that the sacrificial bonding seam which is the thick photoresist layer has been coated with a Cu/Ti (200 nm / 100 nm) seed layer for copper electroplating. The flood exposure was performed and then rinsed in the developer to remove the photoresist in via holes. Copper electroplating with the current density 30 – 40 mA / cm^2 was performed to fill these via holes, and then removed the sacrificial substrate by rinsing in acetone. Note that such a filling process is a bottom-up filling process, and hence the void formation will not happen in the

copper via [12]. Finally, seed layer deposition, photoresist molds patterning and followed copper electroplating with the current density 20 mA / cm^2 on both sides of the glass wafer was performed to form the meandered lines.

The schematic setup of the electroplating experiment was shown in Fig. 4-4, and Fig. 4-5 shows the photograph of the equipment set up for electroplating experiment. It is hard to have an excellent via-filling process in low copper concentration bath [15]~[17]. Owing to the high copper concentration of the plating bath, the reaction species can be easily transported into the bottom of the via-holes. Therefore high copper concentration solution was used in our experiments for via-filling process. The SEM photograph of the cross section view of the via-hole is shown in Fig. 4-6. Besides, from our experimental results, higher growth rate can be observed for larger via-hole. It is because that as the diameter of the via-hole is larger, the copper ions can diffuse into the via-hole easier and hence the electrolyte inside the via-hole is refreshed more often.

From the above descriptions, we can conclude that such compact 3-D MEMS monopole antenna not only has the benefits of simple structure and easy to design but also has the benefit of low cost due to its batch process. In addition, the resonant frequency can be tuned by its total length; hence, a multi-band antenna is also achievable [13]. Figure 4-7 shows the photograph of the 3D monopole antenna, where a meandered copper line with CPW-fed configuration can be seen on the transparent glass substrate.

4-3. Results and Discussion

4-3.1 Return Loss of the 3D Monopole Antenna

The computed and measured input return loss S_{11} of the designed and fabricated MEMS monopole antenna is illustrated in Fig. 4-8. The results are in excellent agreement, depicting a resonance at 2.4GHz and a 190MHz (7.9%) bandwidth, which easily meet the requirement for operation in the 2.4GHz ISM band. Note that there is a slight difference of the S_{11} value between the simulated and measured results, which is probably due to the fabricated metal thickness and dimensions obtained from the copper electroplating process, deviated from the designed values.

4-3.2 Antenna Radiation Characteristics

The radiation characteristics of the designed and fabricated antennas have also been measured in the X-Z plane, X-Y plane and Y-Z plane. The measurement setup of radiation pattern of this 3D monopole antenna is under far field $R \geq 2D^2 / \lambda$ condition (see Fig. 4-9). Note that R is the distance between the horn antenna and the membrane antenna, D is the maximum length of the membrane antenna, and λ denotes the wavelength. The radiation patterns of E-plane and H-plane were measured by the horn antenna while rotating the 3D monopole antenna along the theta and phi directions. Note that E-theta denotes the radiation patterns of E-plane measured along the theta direction, and E-phi denotes the radiation patterns of the E-plane measured along the phi direction.

The radiation characteristics of this monopole antenna system at 2.45GHz for the two principal plane cuts (X-Z, Y-Z and X-Y) are shown in Fig. 4-10. From Fig. 4-10, we can find that the omni-directional radiation pattern of the fabricated monopole antenna is similar to a monopole antenna with z-axial orientation. This is because that the currents which flow along the z-axial directions on the meander line contribute constructively to the field in the E-plane. On the contrary, the adjacent x-oriented currents almost contribute nothing to radiation because of their opposite flowing directions, I(x) and I(-x), on the meander line (as shown in Fig. 4-11). The EM fields generated from I(x) and I(-x) almost neutralized due to the small distance between them. It is the same situation in the z-axial direction. The total electric field for both computed and measured results are normalized with respect to its maximum uniform azimuth cut, and plotted with a maximum gain of 3.4dBi. In addition, the proposed antenna on Pyrex 7740 glass substrate has the possibility of using low temperature anodic bonding to silicon IC wafer, thus the forming of system on package (SoP) module is possible.

4-4. Silicon-Based 3D Antenna

4-4.1 Silicon-Based Dimensions

In order to demonstrate the integration of this 3-D monopole antenna with silicon wafer directly. We based on the design concepts that have mentioned above, another antenna with the same design but different dimensions had been designed successfully on a silicon wafer. The schematic diagram and topology of the proposed antenna are shown in Fig. 4-12. Note that there are two dimensions, A and B, in this design.

4-4.2 Silicon-Based Fabrication Process

The process flow of the silicon-based 3-D monopole antenna was shown in Fig. 4-13. A double polished silicon wafer was cleaned and patterned with inductively coupled plasma reactive ion etching (ICPRIE) for via hole formation. After via hole formation, a layer of S_3N_4 was deposited on the both sides of the wafer with plasma enhanced chemical vapor deposition (PECVD) for electric isolation. The silicon wafer was then bonded with a photoresist (PR) layer (AZ 9260, 5 μm) to a sacrificial substrate which can be dissolved in acetone. The bonded glass wafer was baked on the hot plate at 90 ℃ for 5 minutes. Note that the sacrificial substrate has been coated with a Cu/Ti (200 nm / 100 nm) seed layer for copper electroplating. The flood exposure was performed and then rinsed in the developer to remove the photoresist in via holes. Copper electroplating with the current density 30 – 40 mA / cm^2 was performed to fill these via holes, and then removed the sacrificial substrate by rinsing in acetone. Note that such a filling process is a bottom-up filling process, and hence the void formation will not happen in the copper via. Finally, seed layer deposition, photoresist molds patterning and followed copper electroplating with the current density 20 mA / cm^2 on both sides of the glass wafer was performed to form the meandered lines.

4-5. Conclusions

In this chapter, we demonstrated a novel compact three-dimensional MEMS antenna for WLAN (802.11b). It was fabricated in the form of a folded meander line on both the top and bottom surfaces of the substrate in order to achieve smaller size and wider bandwidth compared to traditional microstrip antenna. Measured performances of the fabricated antenna are in good agreement to the designed values in terms of operating frequency at 2.45 GHz and bandwidth of 190 MHz. Moreover, the resonant frequency can be tuned by its total length; hence, a multi-band antenna is achievable. This small size low cost simple fabrication antenna technology is suitable for mobile communication systems applications.

The antenna can also be combined with micro switches or relays which are used to connect or break electric path, to change the resonance length of the antenna and hence frequency tuning can be achieved, as illustrated in Fig. 4-14. A micro switch/relay with simple silicon-based process has been investigated by us, as discussed in Future Study. The micro switches/relays will be used to construct a phase delay line or phase shifter that can be integrated with the proposed 3-D monopole antenna to form a beam steering antenna or reconfigurable antenna on the same substrate.

4-6. References

[1] W.-C. Liu, “Broadband dual-frequency meandered CPW-fed monopole antenna”, Electron. Lett., 14Th Oct. 2004 Vol. 40 No. 21, pp. 1319 – 1320.

[2] J. Guterman et al, “Dual-band miniaturized microstrip fractal antenna for a small GSM 1800 + UMTS mobile handset”, IEEE MELECOM 2004, May 12-15 2004, pp. 499-501.

[3] Rebekka Porath, “Theory of miniaturized shorting-post microstrip antenna”, IEEE Trans. Antennas Propag. Vol. 48 No. 1, Jan. 2000, pp. 41-47.

[4] Cetiner, B.A. et al, “Monolithic integration of RF MEMS switches with a diversity antenna on PCB substrate”, IEEE Trans. Microwave Theory and Tech. Vol. 51 Issue 1, Jan. 2003, pp 332 – 335.

[5] L. Wang et al, “High aspect ratio through-wafer interconnections for 3D-microsystems”, IEEE The Sixteenth Annual International Conference on Micro Electro Mechanical Systems, 2003. MEMS-03 Kyoto, 19-23 Jan. 2003, pp. 634 – 637.

[6] Manabu Tomisaka et al, “Electroplating Cu filling for through-vias for three-dimensional chip stacking”, IEEE Electronic Components and Technology Conference, 2002. Proceedings, 52nd 28-31 May 2002, pp. 1432 – 1438.

[7] Pham N P et al, “A micromachining post-process module for RF silicon technology”, IEDM Technical Digest, 2000, pp. 481-484.

[8] Takeshi Kobayashi et al, “Via-filling using electroplating for build up PCBs”, Electrochimica Acta, 47 (2001), pp. 85-89.

[9] Vaughn N. Johnson et al, “Through wafer interconnects on active pMOS devices”, IEEE Workshop on Microelectronics and Electron Devices, 2004, pp.82 – 84.

[10] Eugene M. chow et al, “Process compatible polysilicon-based electrical through-wafer interconnects in silicon substrates”, IEEE J. Microelectromechanical Systems Vol. 11 No. 6 Dec. 2002, pp. 631-640.

[11] Xinghua Li et al, “Fabrication of high-density electrical feed-through by deep-reactive-ion etching of Pyrex glass”, IEEE J. Microelectromechanical systems Vol. 11 No. 6 Dec. 2002, pp 625-630.

[12] N T Nguyen et al, “Through-wafer copper electroplating for three-dimensional interconnects”, J. Micromech. Microeng. 12 (2002), pp. 395-399.

[13] Chien-Jen Wang et al, “Small microstrip helical antenna”, IEEE 1999 Asia Pacific Microwave Conference Vol. 2 1999, pp 367 – 370.

[14] Fa-Shian Cheng et al, “Folded meandered-patch monopole antenna for triple-band operation”, IEEE Antennas and Propagation Society International Symposium, Volume 1, 22-27 June 2003, pp. 278 – 281.

[15] Rockwood Electrochemicals Asia Ltd, Taiwan, R.O.C.

[16] Mark Lefebvre et al, “Copper electroplating technology for microvia filling”, Circuit World 2003 Vol. 29 No. 2, pp. 9 – 14.

[17] Cheng-Ching Yeh et al, “Micro via filling plating technology for IC substrate applications”, Circuit Word 2004 Vol. 30 No. 3, pp. 26 – 32.

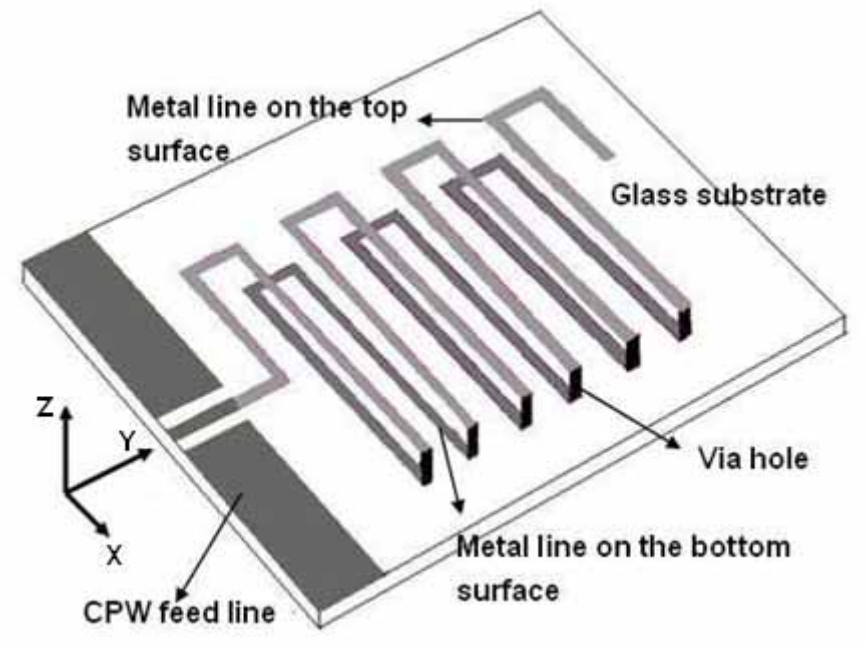

(a)

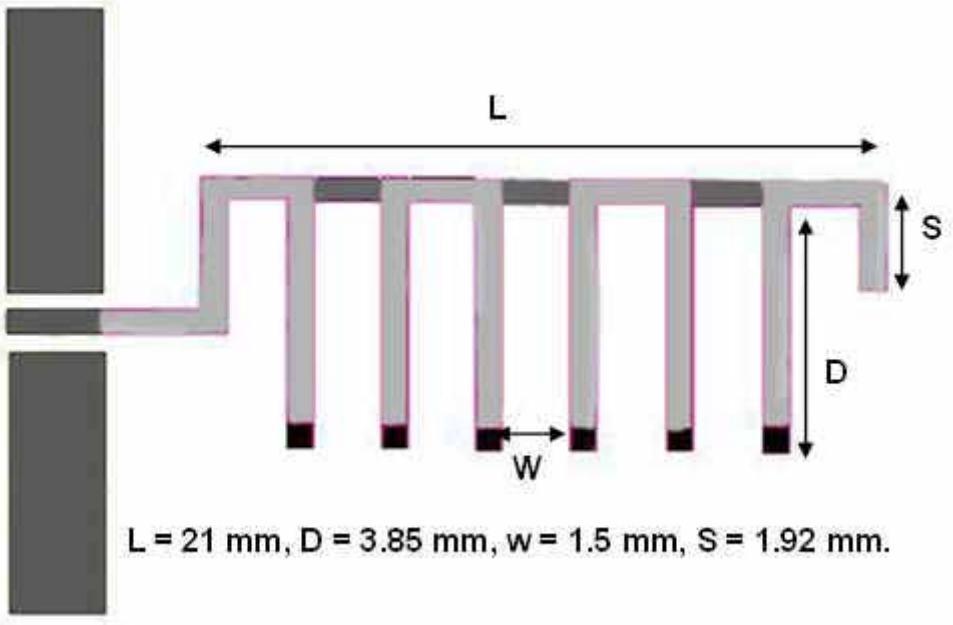

(b)

Figure 4-1: (a) the structure of the 3-D MEMS monopole antenna, (b) Top view of the antenna. (Not to scale)

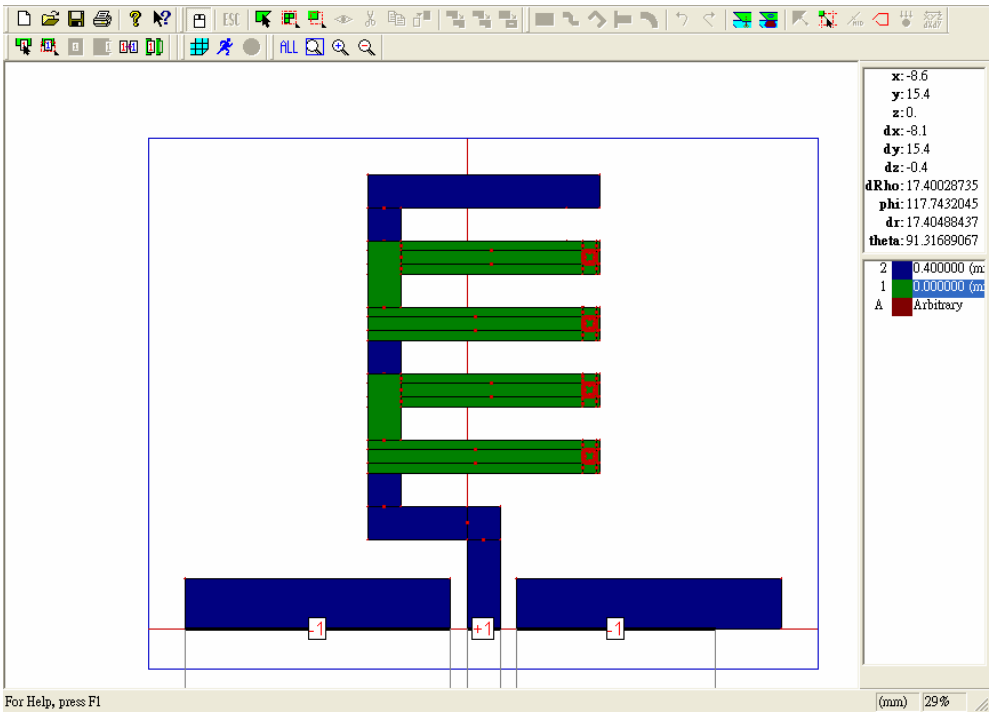

(a)

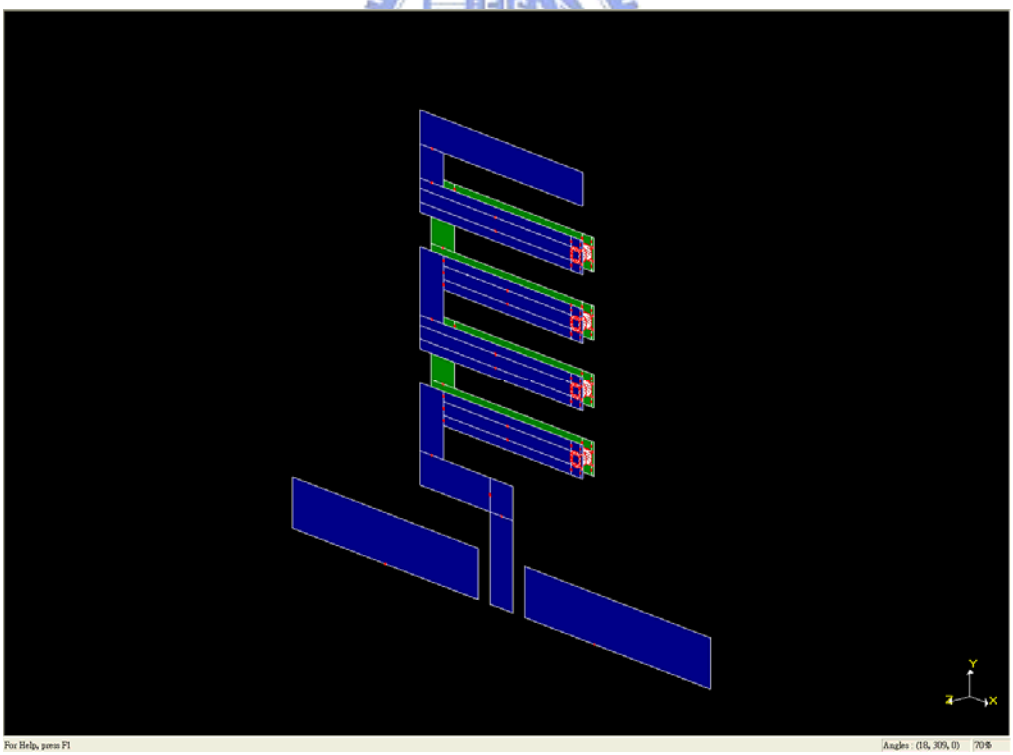

(b)

Figure 4-2: Simulation of the 3D monopole antenna.

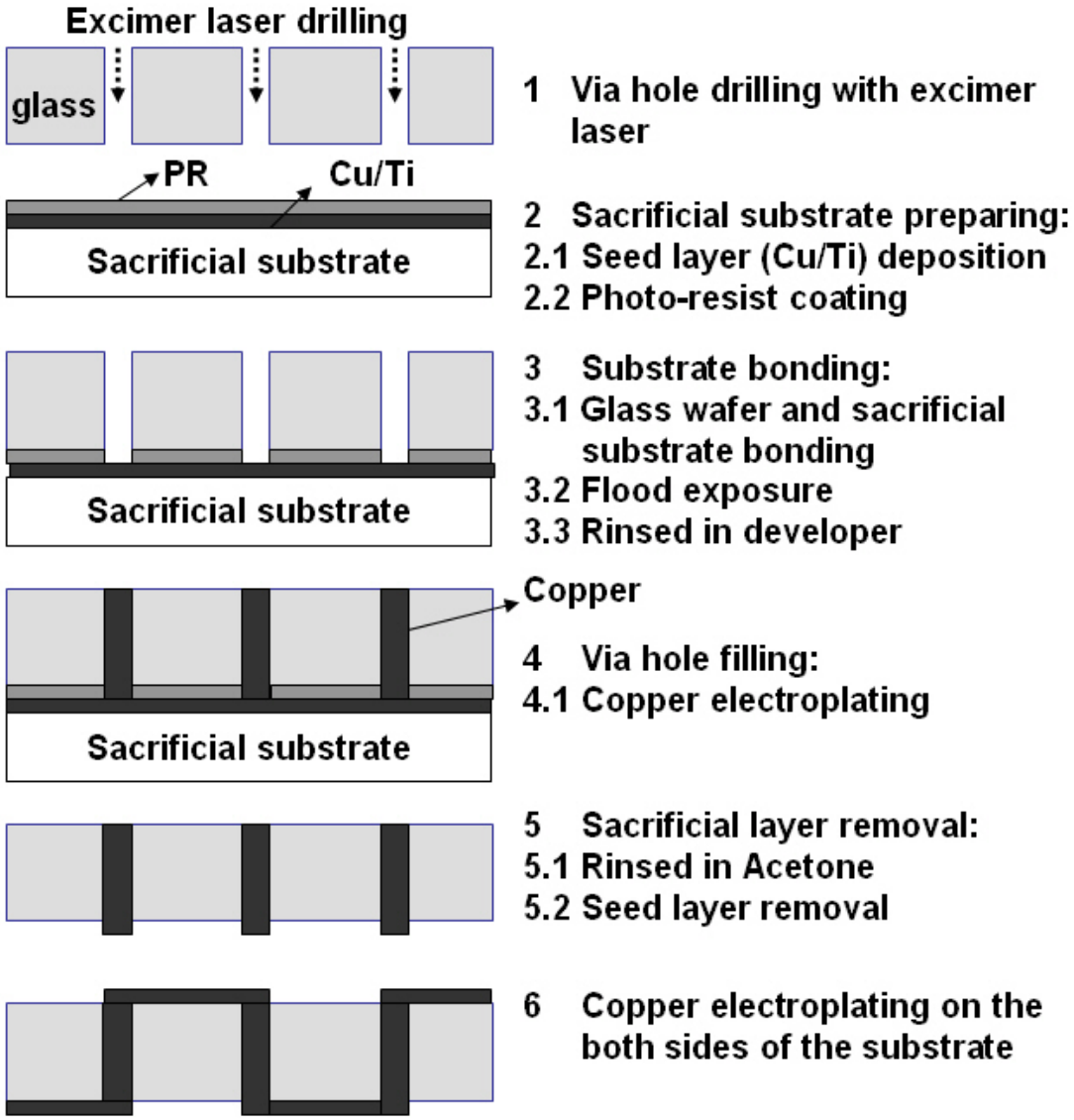

Figure 4-3: the process flow of the 3-D MEMS helical meander antenna.

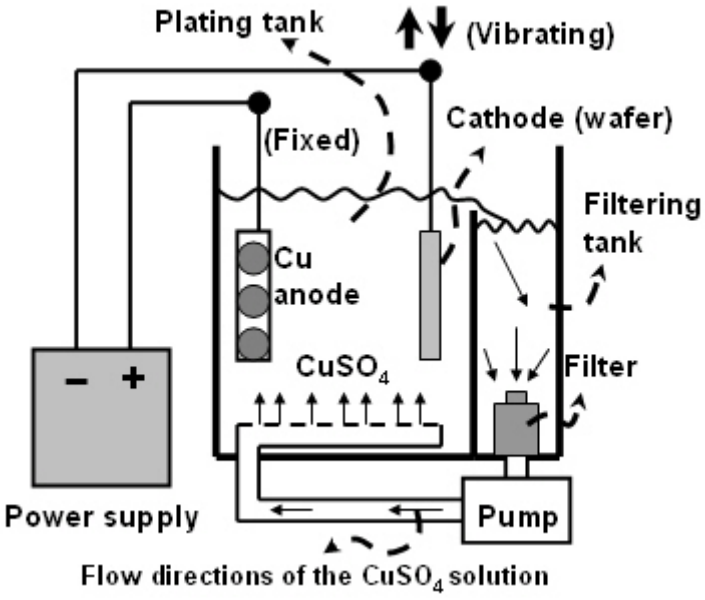

Figure 4-4: The schematic set of the electroplating equipment.

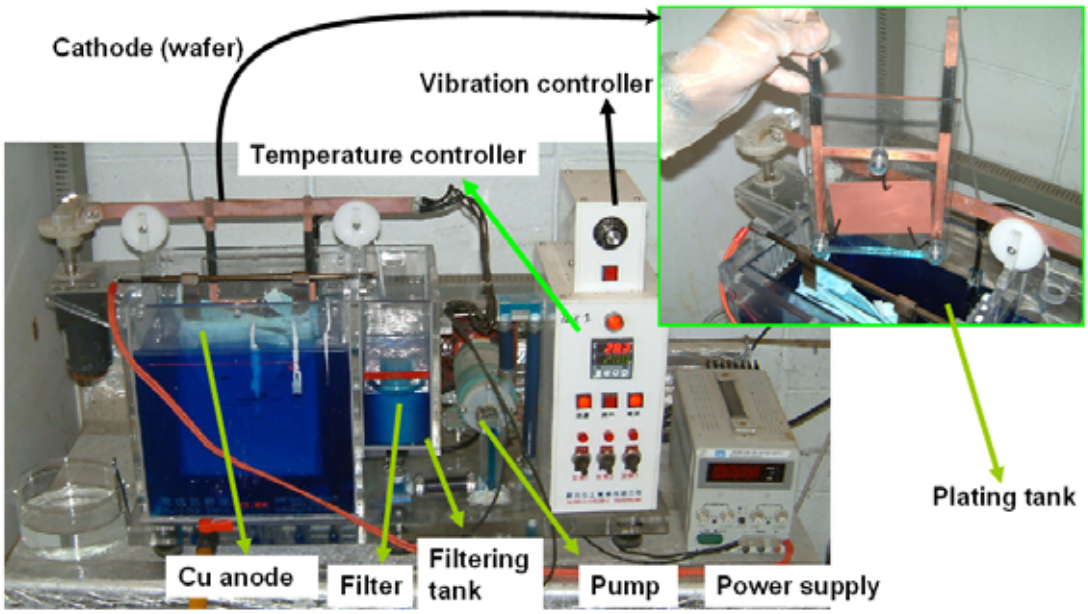

Figure 4-5: The photo of the equipment for electroplating experiment.

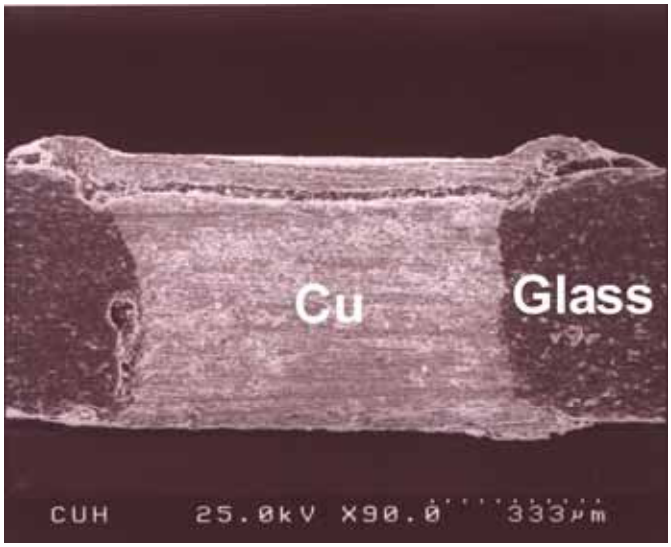

Figure 4-6: The SEM photograph of the cross section of the copper via.

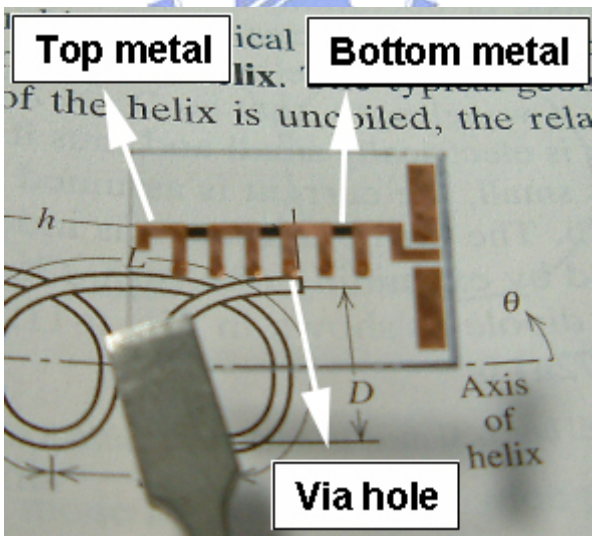

Figure 4-7: The photograph of the 3D monopole antenna.

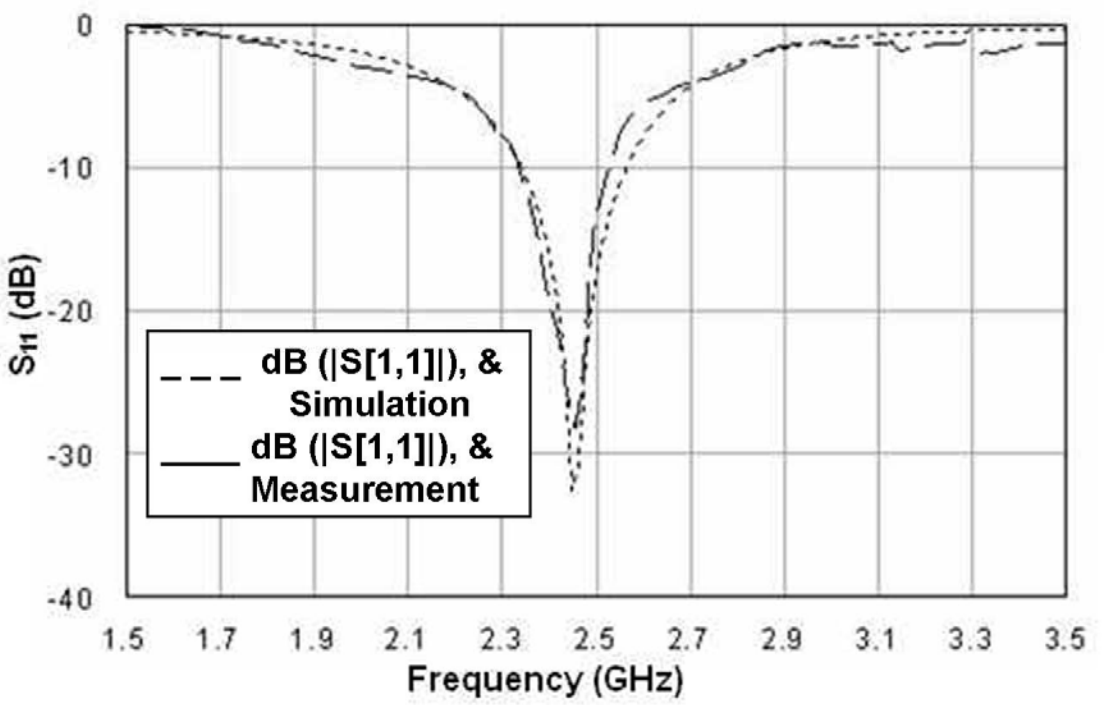

Figure 4-8: Measured and simulated return losses for the proposed antenna.

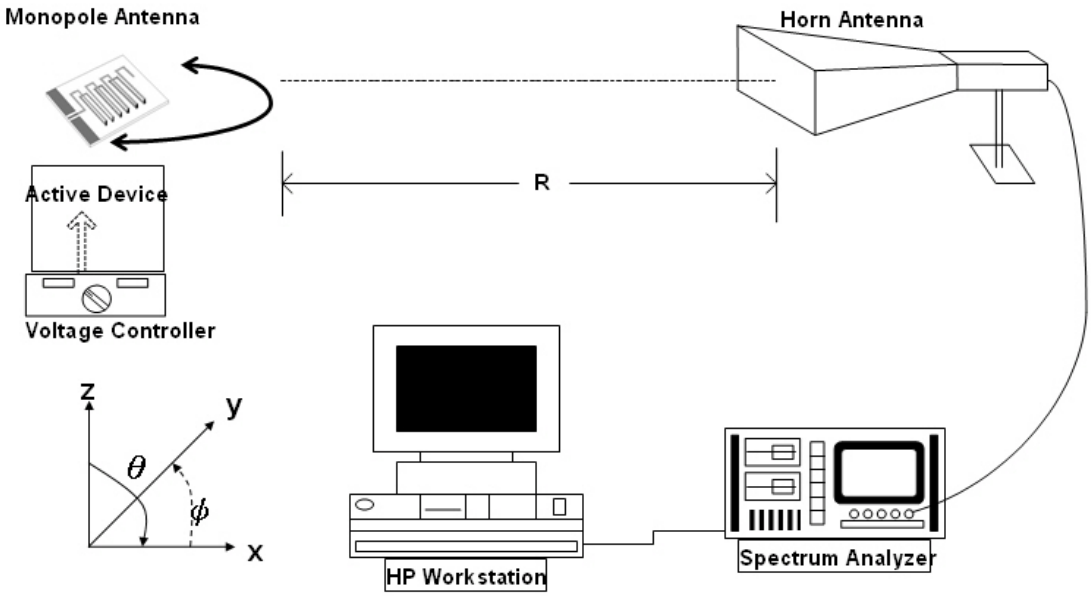

Figure 4-9: The setup for radiation pattern measurement.

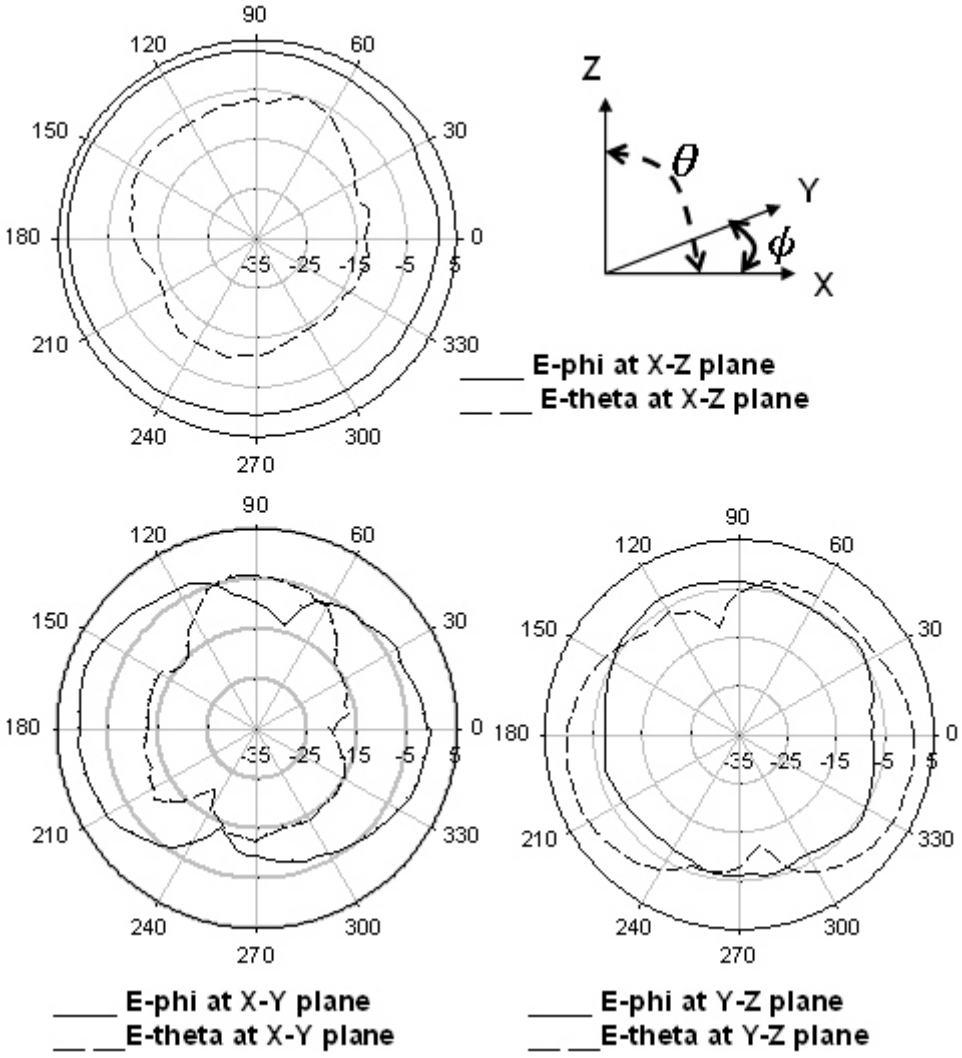

Figure 4-10: Measured radiation patterns for the proposed antenna.

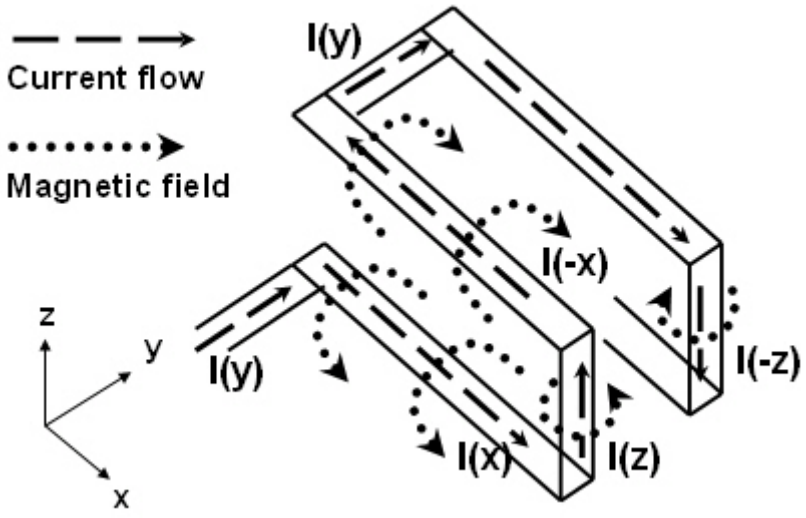

Figure 4-11: EM fields neutralization between adjacent lines.

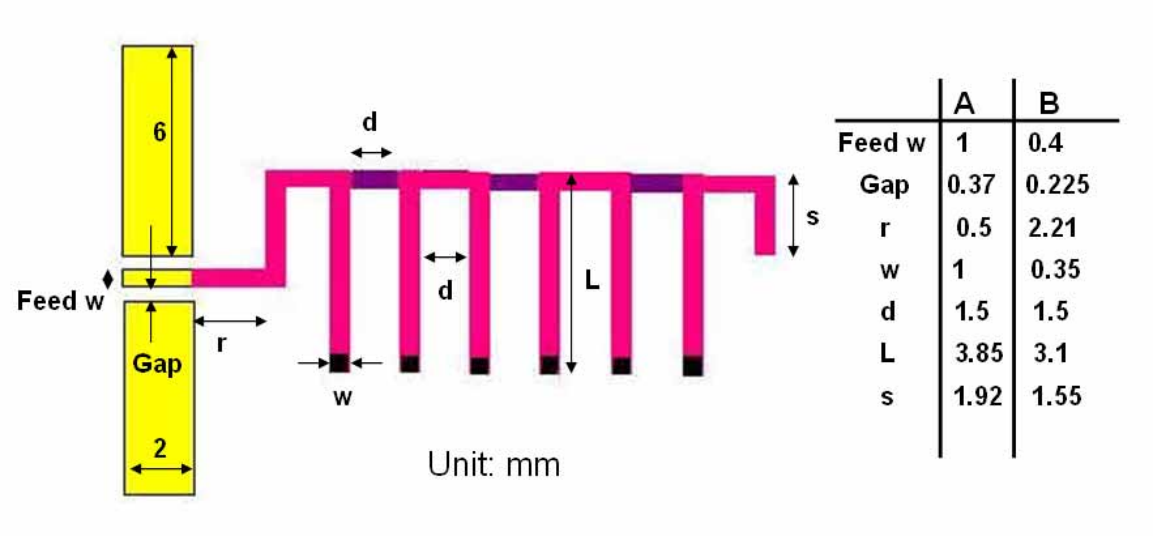

	A	B
Feed w	1	0.4
Gap	0.37	0.225
r	0.5	2.21
w	1	0.35
d	1.5	1.5
L	3.85	3.1
s	1.92	1.55

Figure 4-12: The structure of the 3D antenna on silicon base

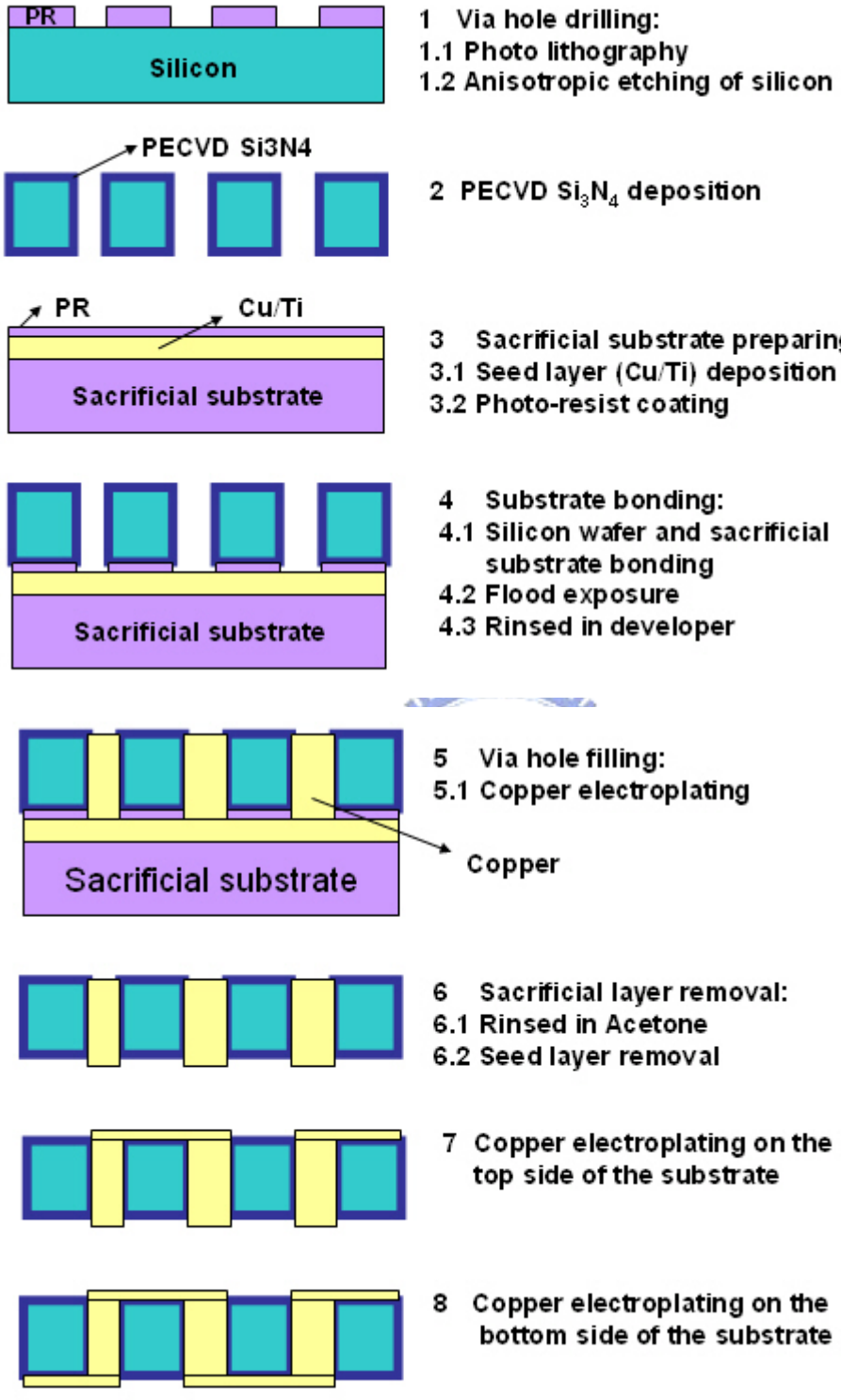

Figure 4-13: The process flow of the 3-D MEMS helical meander antenna.

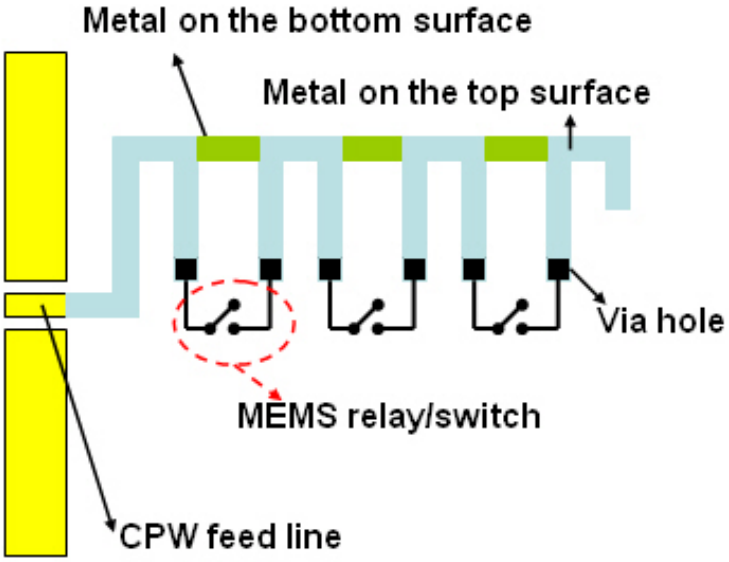

Figure 4-14: Frequency-tunable 3-D MEMS monopole antenna.